

Article

Mining Waste as an Eco-Friendly Adsorbent in the Removal of Industrial Basazol Yellow 5G Dye and Incorporation in Mortars

Mariane Hawerth¹, Eduardo Pereira² , Lariana Negrão Beraldo de Almeida³ ,
Ramiro José Espinheira Martins^{4,5,6}  and Juliana Martins Teixeira de Abreu Pietrobelli^{1,*} 

¹ Postgraduate Program in Chemical Engineering, Department of Chemical Engineering, Federal University of Technology–Parana, Rua Doutor Washington Subtil Chueire, 330, Ponta Grossa 84017-220, Brazil; mari.hawerth@gmail.com

² Postgraduate Program in Materials Science and Engineering, Department of Civil Engineering, State University of Ponta Grossa, Av. Carlos Cavalcanti, 4748, Ponta Grossa 84030-900, Brazil; eduardopereira@uepg.br

³ Postgraduate Program in Chemical Engineering, Department of Chemical Engineering, State University of Maringá, Av. Colombo, 5790, Maringá 87020-900, Brazil; beraldolariana@gmail.com

⁴ Superior School of Technology and Management, Bragança Polytechnic University, Campus de Santa Apolónia, 5300-253 Bragança, Portugal; rmartins@ipb.pt

⁵ LSRE-LCM—Laboratory of Separation and Reaction Engineering—Laboratory of Catalysis and Materials, Faculty of Engineering, University of Porto, Rua Doutor Roberto Frias, 4200-465 Porto, Portugal

⁶ ALICE—Associate Laboratory in Chemical Engineering, Faculty of Engineering, University of Porto, Rua Doutor Roberto Frias, 4200-465 Porto, Portugal

* Correspondence: jpietrobelli@utfpr.edu.br

Abstract: The circular economy seeks to better use materials and minimize waste generation. This article evaluated the use of granite rock powder, a mining residue, as an adsorbent for the Basazol Yellow 5G (BY5G) dye and the reuse of the residue generated by the by treating this effluent in construction products. Characterization of the adsorbent material by N₂ physisorption indicated a surface area of 1514 m² g⁻¹. Energy-dispersive spectrometry (EDS) and X-ray diffraction (XRD) confirmed the presence of silica in the sample and the absence of amorphous halos. The kinetic study showed a removal of approximately 98% at 298 K, and the pseudo-second-order model obtained the best fit. The adsorption isotherm satisfied the Langmuir model and was consistent with the L-type isotherm. The negative value of the Gibbs energy (ΔG°) and the positive value of the enthalpy (ΔH°) indicate that the process is spontaneous and endothermic. The activation energy (E_a) indicates the occurrence of chemical adsorption. The desorption rate was low for the adsorbate, demonstrating the possibility of using residual adsorbent material as a filler in mortar and concrete. The material did not exhibit pozzolanic characteristics and, even after adsorption, it showed favorable results when replacing 10% of the cement with GRP viable for use in civil construction even after the adsorption process.

Keywords: adsorption; cement; circular economy; effluent; granitic rock powder; paper industry



Citation: Hawerth, M.; Pereira, E.; de Almeida, L.N.B.; Martins, R.J.E.; Pietrobelli, J.M.T.d.A. Mining Waste as an Eco-Friendly Adsorbent in the Removal of Industrial Basazol Yellow 5G Dye and Incorporation in Mortars. *Processes* **2023**, *11*, 3349. <https://doi.org/10.3390/pr11123349>

Academic Editors: Maria Angélica Simoes Dornellas De Barros and Thiago Peixoto De Araújo

Received: 2 November 2023

Revised: 23 November 2023

Accepted: 29 November 2023

Published: 1 December 2023



Copyright: © 2023 by the authors. Licensee MDPI, Basel, Switzerland. This article is an open access article distributed under the terms and conditions of the Creative Commons Attribution (CC BY) license (<https://creativecommons.org/licenses/by/4.0/>).

1. Introduction

The circular economy aims to replace the linear model with a circular production model to reduce industrial waste generation and use resources more efficiently [1,2]. One of the practices that can be adopted to contribute to this model is using these residues in other processes, thus avoiding resource wastage. In addition, water reuse helps to reduce the demand for water resources and helps to close the urban and industrial water cycle [3].

In Brazil, numerous quarries have exploited rocks for civil construction and agriculture. The detonation of these rocks in the crushing process generates a powdery material corresponding to 20–25% of the total crushing production [4]. Granitic rock powder (GRP),

a mining waste, mainly consists of quartz (SiO_2) and feldspars [5]. A fraction of this material has applications in civil constructions. However, the large volume produced demands alternative destinations in order not to cause damage to the environment near the storage sites, such as the silting up of rivers and dust [6].

In this context, several studies have been conducted with the purpose of identifying alternative applications for rock dust, with an emphasis on the practice of rock rocking. In this technique, under appropriate conditions, rock dust is applied to the soil as a source of nutrients [7,8]. Another strand of research that explores various applications of rock powder concerns the treatment of effluents, including its use as an adsorbent of phosphate ions in water [9], and as a nickel adsorbent [10].

Dyes are widely used in industries such as textiles, paper, cosmetics, plastic, food, and paint. In the molded pulp industry, dyes are usually added during the pulp preparation stage to color packages [11]. When excess water is extracted during the molding step, the resulting effluent exhibits coloration and requires proper treatment. This is essential due to the vivid colors typically associated with the dyes used in paper, which can potentially pose risks to the aquatic environment and human health [12].

The dye selected for this study belongs to the class of methine dyes, specifically the cyanine type, being widely used to dye paper fibers, including, in the study by Knuston (2004), the author describes that this dye was widely used to dye telephone directories whose pages were traditionally yellow [13]. In addition, the manufacturer of the dye under study stated that the BY5G dye is toxic to aquatic organisms and can cause long-term environmental damage if not treated appropriately.

Adsorption is a simple and efficient effluent treatment method [14] that is frequently used to remove dyes and is characterized by the retention of a chemical species by an adsorbent in the solid phase [15]. The choice of the adsorbent directly affects the viability and efficiency of the adsorption process. Therefore, adsorbent materials with high surface areas and low cost are generally used [16,17].

The use of granitic rock powder as an adsorbent material in the treatment of molded pulp effluent with dye is attractive due to the alternative destination of pulverulent material and because it makes the adsorption process cheaper. However, after adsorption, the residual adsorbent material loses its usefulness in adsorbate removal and must be discarded. In civil construction, it is common to use mineral additions to replace cement in mortars and concretes to improve the resistance performance and reduce the use of clinker in Portland cement, which is responsible for the emission of thousands of tons of CO_2 [18,19]. Studies by Assaad et al. (2021) [20] and AlArab et al. (2020) [21] have highlighted the positive impacts of replacing both fine aggregates and cement with waste materials.

Mineral additions can exhibit pozzolanic characteristics or act as fillers. Pozzolanic materials comprise materials with no or low crystallinity, which when in contact with water, react with calcium hydroxide and exhibit cementing properties [22]. Materials that do not present pozzolanicity can act as fillers, which are characterized as finely divided materials [23] and exert a physical effect. The filler reduces the porosity of the system by filling voids and improving the durability of the concrete or mortar [22,23].

Therefore, granitic rock powder has the potential to be used as a filler in mortars [24] and is an eco-friendly alternative for the subsequent disposal of residual adsorption materials. In addition to the reuse of mining waste, the implementation of an efficient treatment that enables the reuse of water in industrial processes is essential to guarantee the quality of the packaging produced, minimize the demand for water resources, and allow for the disposal of the effluent in the ecosystem within the standards required by environmental laws. In this circular economy context, this study aimed to evaluate the removal of the BY5G dye by GRP from synthetic effluents in batch and the reuse of the adsorption residue in mortars.

2. Materials and Methods

2.1. Preparation of the Adsorbent and Synthetic Solution Dye

The granitic rock powder (GRP) used in this study was obtained from a mining company and the BY5G dye by a molded pulp company, both from Campos Gerais, Paraná, Brazil. The material was dried in an air-circulating oven with air renewal (SL 102—SOLAB, Piracicaba, Brazil) at 303 K for 24 h and sieved through a 200 mesh to obtain the passing material. Synthetic BY5G dye solutions were prepared using distilled water, and the pH was adjusted using NaOH and HCl solutions at 0.1 M.

2.2. Characterization of the Adsorbent

2.2.1. N₂ Physisorption

The specific area (S_0), pore volume (V_p), and mean pore diameter (d_p) properties of the GRP were determined by N₂ physisorption at 77 K using Novatouch 2LX, Quantachrome equipment. The specific area (S_0) was calculated using the Brunauer (Emmett) Teller method.

2.2.2. FTIR

The functional groups of the GRP before and after the adsorption process were identified via analysis using a Fourier transform spectrophotometer (IRPrestige-21, Shimadzu, Kyoto, Japan) in the wavelength range of 4000 to 400 cm⁻¹, with a resolution of 2 cm⁻¹.

2.2.3. SEM and EDS

Morphological and chemical characterizations of the GRP before and after adsorption were carried out using a scanning electron microscope (VEGAN LMU, Tescan – Koutovice, Czech Republic), and the samples were prepared by depositing a thin layer of gold and palladium. The analysis was performed at a voltage of 20 kV and a magnification of 1000 times. An energy-dispersive spectroscopy (EDS) detector (X-Act, Oxford, UK) was used to identify the chemical elements.

2.2.4. XDR

The mineralogical composition of the GRP (before and after adsorption) was determined by X-ray diffraction using an Ultima IV model diffractometer (Rigaku—Tokyo, Japan) equipped with Cu-K α radiation and operated at 40 kV and 30 mA. The interval adopted for scanning ranged from 5° to 75°, with a step of 0.02° every 60 s.

2.3. Adsorption Experiments

The use of granite rock powder as an adsorbent material in dye-containing effluents is a positive way to dispose of this waste generated by mining. Nevertheless, assessing the efficacy of this residue in effluent treatment via adsorption requires the examination of operational parameters, dye removal efficiency over time, corresponding capacity for removal, and potential for subsequent dye and adsorbent recovery.

In 125 mL Erlenmeyer flasks, 0.15 g of GRP was added to 25 mL of BY5G dye solution at a concentration of 60 mg L⁻¹. The dye and adsorbent in the aqueous solution were kept in contact on a rotating shaker at 130 rpm for 1 h. The effect of the pH was evaluated in the range 1–12.

The amount of BY5G dye removed by GRP was determined using Equations (1) and (2):

$$q_e = \left(\frac{C_0 - C_e}{m} \right) V \quad (1)$$

$$R = \left(\frac{C_0 - C_e}{C_0} \right) \times 100\% \quad (2)$$

where q_e is the amount of adsorbate in the solid phase (mg g^{-1}), V is the volume of the solution (L), C_0 is the initial concentration of adsorbate in the solution (mg L^{-1}), C_e is the concentration of adsorbate in the solution (mg L^{-1}), m is the mass of adsorbent (g), and R is the dye removal (%).

Adsorption tests were performed in a batch system.

2.4. Kinetic Studies

Experiments were performed to investigate the equilibrium time, which is important for determining the variation in the efficiency over time. These results allow us to determine how long it is necessary to keep the GRP in contact with the effluent to carry out the adsorption treatment. In 125 mL flasks, 0.15 g of granitic rock powder was used for 25 mL of the synthetic solution of 60 mg L^{-1} at 130 rpm. The remaining dye concentrations were evaluated from 0 to 360 min at temperatures of 298, 303, 313, and 323 K. For this purpose, the samples were centrifuged and read in a UV-Vis spectrophotometer after the contact time. Pseudo-first-order [25], pseudo-second-order [26], and Elovich [27] models were fitted to the experimental data by Equations (3), (4), and (5), respectively:

Pseudo-first-order

$$\log(q_{eq} - q_t) = \log(q_{eq}) - \left(\frac{k_1}{2.303}\right)t \quad (3)$$

Pseudo-second-order

$$\frac{t}{q_t} = \frac{1}{k_2 q_{eq}^2} + \frac{1}{q_{eq}} t \quad (4)$$

Elovich

$$q_t = \frac{1}{\beta} \ln(\alpha\beta) + \frac{1}{\beta} \ln(t) \quad (5)$$

where q_{eq} is the amount of adsorbate adsorbed at equilibrium per gram of adsorbent (mg g^{-1}), q_t is the amount of adsorbate adsorbed in a certain time t per gram of adsorbent (mg g^{-1}), k_1 is the adsorption rate constant of the pseudo-first-order kinetic model (min^{-1}), k_2 is the adsorption rate constant of the pseudo-second-order kinetic model ($\text{g mg}^{-1} \text{min}^{-1}$), α is the initial adsorption rate for the Elovich model ($\text{mg g}^{-1} \text{min}^{-1}$), β is the desorption constant for the Elovich model (mg g^{-1}), and t is the time (min).

2.5. Equilibrium Studies

The adsorption capacity of the GRP for the BY5G dye was evaluated using the equilibrium test. The isotherms were determined by the ratio between the amount of dye adsorbed per mass of adsorbent (mg g^{-1}) and the concentration of the synthetic dye solution at equilibrium (mg L^{-1}). The experimental data from temperatures of 298, 303, 313, and 323 K were applied to the linear Langmuir (Equation (6)) and Freundlich (Equation (7)) isotherm model [28].

Langmuir

$$\frac{C_{eq}}{q_{eq}} = \frac{1}{q_{max} k_L} + \frac{C_{eq}}{q_{max}} \quad (6)$$

Freundlich

$$\ln q_{eq} = \ln k_F + \frac{1}{n_F} \ln C_{eq} \quad (7)$$

where q_{eq} is the amount of adsorbate adsorbed per gram of adsorbent at equilibrium (mg g^{-1}), q_{max} is the maximum adsorption capacity in the monolayer (mg g^{-1}), k_L is the Langmuir constant (L mg^{-1}), C_{eq} is the remaining adsorbate concentration in the equilibrium solution (mg L^{-1}), k_F is the dimensionless Freundlich constant related to the adsorption capacity, and n_F is the dimensionless Freundlich constant related to the adsorption intensity.

2.6. Thermodynamic Analysis

Thermodynamic analysis was useful for determining the nature of the process, its spontaneity, and whether it occurs endothermically or exothermically. The Gibbs free energy (ΔG°_{ads}), enthalpy (ΔH°_{ads}), and entropy (ΔS°_{ads}) [29,30] were calculated using Equations (8)–(10):

$$\Delta G^\circ_{ads} = \Delta H^\circ_{ads} - T\Delta S^\circ_{ads} \quad (8)$$

$$\ln k_d = -\frac{\Delta H^\circ_{ads}}{RT} + \frac{\Delta S^\circ_{ads}}{R} \quad (9)$$

$$k_d = \frac{q_{eq}}{C_{eq}} \quad (10)$$

where q_{eq} is the amount of adsorbate adsorbed per gram of adsorbent at equilibrium (mg g^{-1}) and C_{eq} is the concentration of adsorbate remaining in the solution at equilibrium (mg L^{-1}).

The activation energy determines the minimum energy required for the reaction and can be obtained from the kinetic data at different temperatures. This parameter assists in verifying the occurrence of physical or chemical adsorption by the Arrhenius equation. Using the data from the kinetic model that best described the adsorption process, the Arrhenius equation is given by Equation (11):

$$\ln(k_2) = \ln(A) - \frac{E_a}{RT} \quad (11)$$

where k_2 is the pseudo-second-order kinetic constant ($\text{g mg}^{-1} \text{g}^{-1}$), A is the Arrhenius constant ($\text{g mg}^{-1} \text{g}^{-1}$), E_a is the activation energy (kJ mol^{-1}), R is the universal ideal gas constant ($8.314 \text{ J mol}^{-1} \text{ K}^{-1}$), and T is the temperature (K).

2.7. Desorption Studies

A desorption test was carried out to evaluate the possibility of recovering adsorbed dye. In 125 mL Erlenmeyer flasks, 0.15 g of GRP with adsorbed dye was placed in contact with six different eluents (distilled water, ethyl alcohol 50% *v/v*, HCl 0.1 M, HCl 0.01 M, NaOH 10^{-6} M, and NaOH 10^{-7} M) at 130 rpm, 298 K for 4 h. Subsequently, the samples were centrifuged and analyzed using a UV-Vis spectrophotometer. The GRP with adsorbed dye was obtained from the batch adsorption test. The amount of desorbed dye and percentage of desorption are given by Equations (12) and (13), respectively:

$$q_{ed} = \frac{V_{el}(C_{ed})}{m_{sd}} \quad (12)$$

$$P_d = \frac{q_{ed}}{q_e} \times 100\% \quad (13)$$

where V_{el} is the eluent volume (L), C_{ed} is the concentration of desorbed dye in the liquid phase (mg L^{-1}), m_{sd} is the mass of adsorbent with dye (g), and q_e is the amount of dye present in the adsorbent material at equilibrium (mg g^{-1}).

2.8. Disposal of Adsorption Residue

After using granite rock powder to remove the BY5G dye, the residue generated by the adsorption treatment also needs to be disposed of in an environmentally friendly manner. To achieve this, it is necessary to evaluate its pozzolanicity and physical mechanical performance for application in a new context: mortars.

2.8.1. Pozzolanic Activity Index (IAP)

To analyze the pozzolanic activity of the GRP with lime after adsorption, four proof bodies (5×10 cm) composed of 104 g of sodium hydroxide, 936 g of sand, 246 g of GRP, and 252 g of water were molded, as described by NBR 5751 [31]. The specimens were ruptured after seven days of curing using a digital electric press with a capacity of 1000 kN LM-02 (Solocap, Minas Gerais, Brazil).

2.8.2. Cement Performance Index

The cement performance index was determined using NBR 5752 [32]. Six specimens composed of cement, sand, and water (reference), and six specimens containing GRP after adsorption (mortar B) were molded. The quantities of the materials used are listed in Table 1.

Table 1. Material for the IAP.

	Cement (g)	Sand (g)	Water (g)	GRP after Adsorption (g)
Reference	624	1872	300	-
Mortar B	468	1872	300	156

The specimens were broken after 28 d of curing in a digital electric press with a capacity of 1000 kN LM-02 (Solocap).

2.8.3. Compressive and Tensile Strength Test

To evaluate the behavior of the partial replacement of cement by GRP after adsorption, aiming at the correct final destination of the adsorbent used in the removal of the BY5G dye, the specimens were prepared with substitutions of 5%, 10%, 15%, and 20%. For the reference specimens, 500 g of cement and 153 g of water were used to obtain a w/c ratio of 0.31, which was maintained for different replacements, as shown in Table 2.

Table 2. Material for cement paste.

	GRP (g)	Cement for GRP (g)	GRPA (g)	Cement for GRP (g)	Water (g)
5%	22.67	477.33	22.84	477.16	153
10%	45.34	454.66	45.69	454.31	
15%	68.02	431.98	68.53	431.47	
20%	90.69	409.31	91.38	408.62	

The compressive strength test followed NBR 7215 [33] and the tensile strength by diametral compression followed NBR 7222 [34], immersion absorption and void index NBR 9778 [35]. In both tests, four specimens were molded using cement, sand, water, and GRP after adsorption and four reference specimens were molded using only cement, sand, and water. The specimens were broken using a DL 10,000 hydraulic press (Emic brand), after 28 d of curing.

3. Results and Discussion

3.1. Characterization of Adsorbents

3.1.1. N₂ Physisorption

The results of the N₂ physisorption analysis for the GRP showed a specific area (S_0) of $1.514 \text{ m}^2 \text{ g}^{-1}$, pore volume (V_p) of $0.00515 \text{ cm}^3 \text{ g}^{-1}$, and mean pore diameter (d_m) of 6.8 nm, demonstrating a low surface area compared to conventional adsorbents such as activated carbon [36] and zeolites [37]. The adsorption and desorption isotherms of the

GRP (Figure 1) indicate that the material is mesoporous, similar to the type IV and type V isotherms [38].

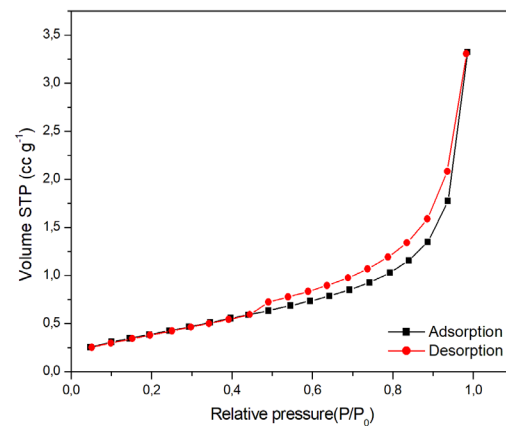


Figure 1. Adsorption/desorption isotherm of granitic rock powder.

3.1.2. FTIR Analysis

The FTIR spectra of the GRP before and after adsorption are shown in Figure 2. It can be observed that the graphs of the samples are similar and that there are several peaks between 3414 and 419 cm^{-1} , marked with a black line. The identification of the functional groups present in the samples helps to understand the adsorption behavior [16]. The most relevant peaks were observed at approximately 3400, 1600, 1100–1000, and 770–400 cm^{-1} . The band at 3414 cm^{-1} is attributed to the O-H and the N-H groups [16,39,40]. Vibrations between 2000 and 1500 cm^{-1} are indicative of double bonds [41]. The peaks between 1680 and 1600 cm^{-1} are related to the presence of C=C bonds of alkenes [39], while vibrations between 1600 and 1450 cm^{-1} imply an aromatic ring [41].

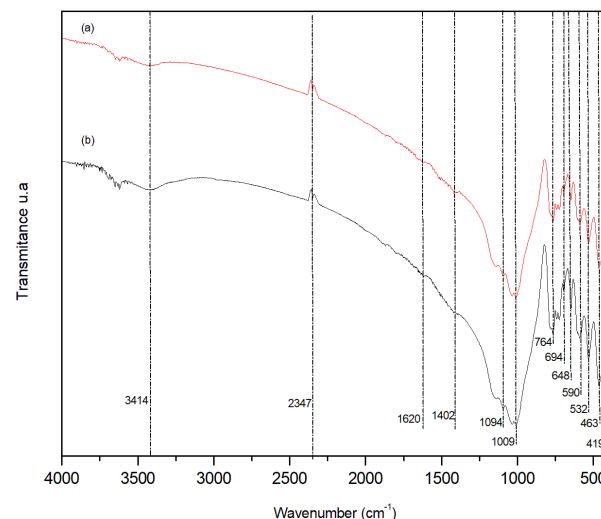


Figure 2. FTIR spectra of granitic rock powder before (a) and after (b) adsorption.

Furthermore, peaks close to 1630 cm^{-1} are attributed to Si-OH binding in the granitic rock samples [42]. The fingerprint region (1500–400 cm^{-1}) is a complex analysis area due to the amount of existing vibrations and the sample variability [43]. Peaks at 1015–1067 cm^{-1} indicate Si-O stretching. The vibrations at 764 cm^{-1} and 532 cm^{-1} indicate the elongation of Al-O-Al and Al-O-Si, respectively. Furthermore, vibrations close to 432 cm^{-1} were associated with Si-O-Si deformation [44].

Despite the lack of access to the molecular structure of the BY5G dye, it is assumed that adsorption occurred between the dye-GRP system and the active group Si-O granitic

rock powder. It is also noted that there is a similarity between the FTIR spectra of the GRP and the GRP after adsorption, indicating that there were no changes in the structure of the material owing to the adsorption process. This result is positive because the GRP retains its original characteristics and demonstrates the robustness of the material to certain processes.

3.1.3. SEM–EDS

The GRP morphology before and after adsorption was analyzed using scanning electron microscopy (SEM) with energy-dispersive spectroscopy (EDS), as shown in Figure 3.

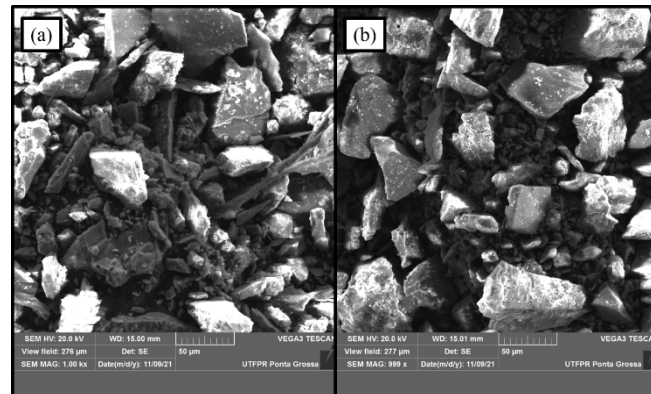


Figure 3. SEM–EDS with 1000x GRP before (a) and after (b) adsorption.

The adsorbent material had particles of different sizes and irregular shapes, similar to those of small pebbles. Furthermore, the adsorption process did not generate significant morphological changes on the sample surface, which was consistent with the FTIR results.

In Table 3, it is possible to compare the EDS results for both the samples.

Table 3. EDS characterization data of granitic rock powder.

Element	GRP Natural (%)	GRP after Adsorption (%)
O	53.9	54.9
Si	29.3	30.5
Al	7.1	6.5
Na	4.0	3.6
K	3.4	2.6
Fe	1.7	1.9

The samples before and after adsorption contained O, Si, Al, Na, K, and Fe. These elements are generally in the form of oxides and are common in granitic rock samples [9]. The predominance of oxygen, silicon, and aluminum classifies these materials as aluminosilicates [45]. The samples demonstrated similar compositions, implying that the dye did not incorporate elements that could be potentially toxic into the samples, enabling the subsequent use of the material after adsorption, such as in mortars.

3.1.4. XDR Analysis

The XRD results indicated the presence of SiO_2 , albite, and microcline in both samples [46], which is in agreement with the EDS results (Figure 4). In addition, the granitic rock powder samples exhibited crystalline characteristics without amorphous halos. This result indicates that the GRP likely acts as a filler to replace the cement in the Portland cement matrix. Both samples had similar mineralogies.

From all the characterization tests conducted on the GRP, it appears that no significant changes were generated in the structure and composition of the material before and after the adsorption process.

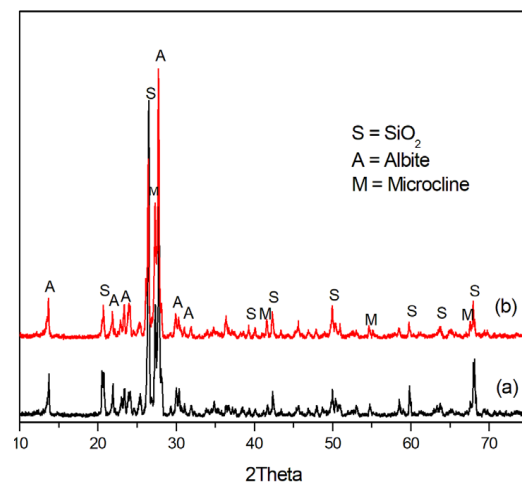


Figure 4. XRD of granitic rock powder before adsorption (a) and after adsorption (b).

3.2. Effect of pH

pH is one of the main factors affecting the adsorption efficiency [16]; therefore, it is important to evaluate its influence on this process. This happens because the pH value of the solutions can influence the removal of pollutants due to the change in the electrical charge of the adsorbent surface [47]. The BY5G dye is cationic in nature; therefore, adsorption is theoretically favored at basic pH values. At pH values of 2, 7, and 12, the removal rates were 92.5%, 95.6%, and 97.9%, respectively, under the operating conditions of 298 K and 130 rpm for 1 h. Despite greater removal at a more basic pH, the resulting difference between the removal percentages can be considered low.

Thus, according to the analysis of the effect of the pH on the adsorption process, the pH did not significantly interfere with the removal of the BY5G by the GRP. Considering these results and the fact that the pH of the industrial effluent under study was close to neutral, a pH of 7 was defined as the optimal operating condition for the kinetic and balance tests. Hence, there is no need for alterations in the pH of the studied effluent, eliminating the need for the industry to incur costs associated with the addition of acids or bases to regulate the pH in the context of implementing adsorption treatment.

3.3. Kinetic Studies

The removal of the BY5G dye over time is shown in Figure 5.

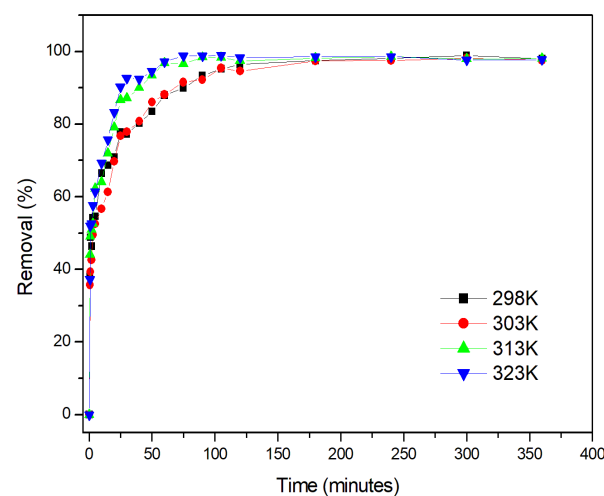


Figure 5. Removal of BY5G dye by granitic rock powder in relation to time.

The results indicated that the maximum removal of the BY5G dye under the tested conditions was similar at all evaluated temperatures. However, equilibrium was reached more quickly as the temperature increased, reaching 240, 180, 60, and 40 min for the temperatures of 298, 303, 313, and 323 K, respectively. In addition, a similar behavior at different temperatures is the rapid removal in the first minutes of the reaction. While the time needed to achieve equilibrium was more favorable at 323 K, the removal of the BY5G at 298 K within 10 min was approximately 70%, eventually reaching equilibrium with a 99% reduction. This demonstrates the effectiveness of GRP as an adsorbent without the need for energy expenditure to increase the system temperature.

The adsorption kinetics were studied by applying the pseudo-first-order, pseudo-second-order, and Elovich kinetic models. Table 4 presents the results.

Table 4. Parameters of kinetic models.

Models	Parameters	Temperature (K)			
		298	303	313	323
Pseudo-first-order	q_e (mg L ⁻¹)	1.9993	1.9419	1.9208	1.8546
	k_1 (min ⁻¹)	0.0325	0.0371	0.0722	0.0833
	R ²	0.9833	0.9539	0.9699	0.9632
Pseudo-second-order	q_e (mg L ⁻¹)	10.1711	9.8708	9.8691	9.3920
	k_2 (min ⁻¹)	0.0264	0.0392	0.0990	0.2397
	R ²	0.9995	0.9997	0.9999	0.9999
Elovich	α (mg g ⁻¹ min ⁻¹)	222.7094	156.2338	843.9453	1069.6420
	β (mg g ⁻¹ min ⁻¹)	1.0709	1.0347	1.1823	1.2505
	q_e (mg L ⁻¹)	10.2297	9.9338	9.3039	8.7065
	R ²	0.9720	0.9690	0.9327	0.9046
Experimental data	q_e (mg L ⁻¹)	10.1235	9.8534	9.8714	9.3441
	t equilibrium (min)	240	180	60	40

The pseudo-second-order model showed the best fit to the experimental data in relation to the pseudo-first-order and Elovich models, with an R² value of 0.99 for all temperatures. The kinetic constants (k_2) of the pseudo-second-order showed increasing importance as the temperature increased, implying a reduction in the time to reach equilibrium. The conformity of the experimental data to the pseudo-second-order kinetic model indicated the occurrence of chemical adsorption [26]. In addition, basic dyes, such as BY5G, have a high substantivity between the dye and adsorbent and suffer from the increased diffusion of molecules at higher temperatures [48], which can be observed in the kinetic results.

3.4. Equilibrium Studies

Changing the initial concentration of the BY5G dye solution allowed for the evaluation of the adsorption equilibrium dynamics. The isotherms enable the theoretical determination of the relation between the adsorbate in the liquid phase and the adsorbent, at a given temperature. The variation between the amount of dye in the solid phase (q_e) and liquid phase (C_e) is shown in Figure 6.

The behavior of the curve was similar for the temperatures under analysis, which showed a gradual increase in relation to C_e until it reached a relatively constant value, approximately 50 to 350 mg L⁻¹. This behavior is typically observed when adsorption occurs in a monolayer [49].

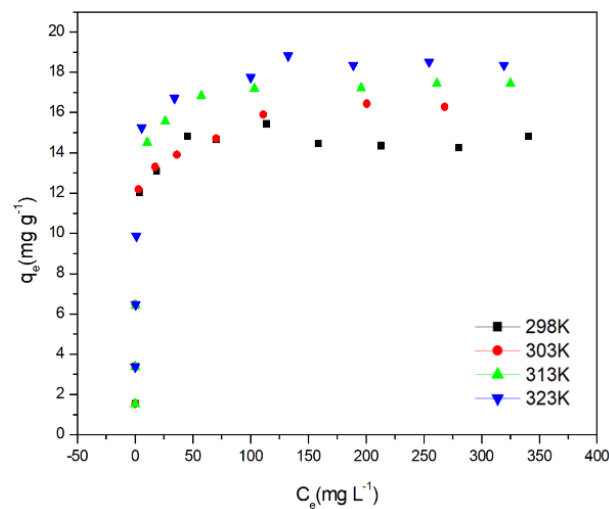


Figure 6. Equilibrium data of adsorption of BY5G dye by granitic rock powder.

The Langmuir and Freundlich adsorption isotherms were evaluated using the equilibrium parameters and correlation coefficients obtained by fitting linear equations to the experimental data, as presented in Table 5.

Table 5. Adsorption isotherm parameters.

Parameters		298 K	303 K	313 K	323 K
Langmuir	q_{max} (mg g ⁻¹)	14.6003	16.6808	17.5156	18.5213
	K (L mg ⁻¹)	2.1183	0.2665	0.5124	0.7039
	R^2	0.9992	0.9997	0.9999	0.9997
Freundlich	k_F (L mg ⁻¹)	2.0241	2.0719	2.1307	2.3890
	n_F	4.4096	4.5229	4.2541	5.3490
	R^2	0.7822	0.7799	0.7339	0.8143

The q_{max} values obtained at different temperatures demonstrated that the maximum adsorption capacity increased with the increasing temperature. This is because an increase in the temperature causes thermodynamic movement that provides a greater number of collisions between the adsorbent adsorbate, which is more favorable for the adsorption reaction [50].

Based on the results, the Langmuir model best described the experimental data, considering R^2 . This model considers the hypothesis that the adsorption of the applications on the surface of the adsorbent occurs uniformly, forming a monolayer covering the surface [25]. The adsorption isotherm of GRP can be classified as an L-type isotherm. This type of curve has a steep slope in the initial instants due to the number of available sites and decreases with the increasing concentration due to the progressive covering of the surface [51].

3.5. Thermodynamic Analysis

The thermodynamic analysis allows for a better understanding of the interaction between the adsorbate/adsorbent during adsorption. The thermodynamic parameters are presented in Table 6.

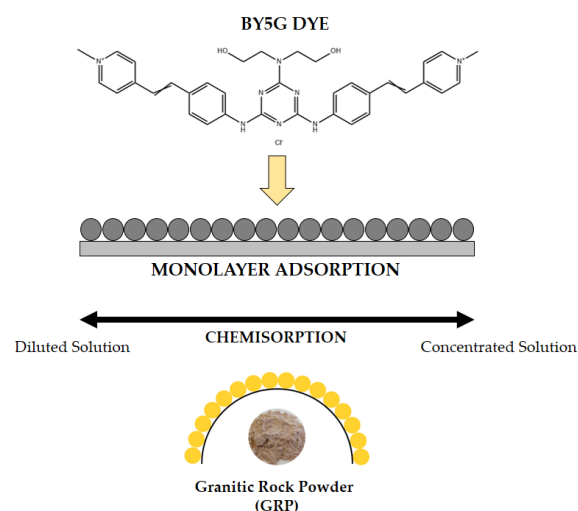
The negative values of the Gibbs energy (ΔG°) indicate that adsorption occurred spontaneously and thermodynamically favorably at all temperatures studied. As the enthalpy change (ΔH°) was positive, the adsorption process can be classified as endothermic. The negative value of ΔS° ($-137.75 \text{ J mol}^{-1} \text{ K}^{-1}$) suggests a decrease in randomness at the solid/solution interface during adsorption.

Table 6. Thermodynamic parameters of BY5G dye adsorption by granitic rock powder.

T (K)	Kd	ΔG° (kJ mol ⁻¹)	ΔH° (kJ mol ⁻¹)	ΔS° (J mol ⁻¹ K ⁻¹)
298	5.30	-4.14	37.06	-137.75
303	6.07	-4.54		
313	10.29	-6.07		
323	16.29	-7.50		

Generally, E_a values of 5 to 40 kJ mol⁻¹ are assigned to physical adsorption and 800 kJ mol⁻¹ for chemical adsorption [52,53]. The activation energy was determined by the data obtained from the graph $\ln(k_2)$ versus $1/T$, resulting in 71.35 kJ mol⁻¹ ($R^2 = 0.9993$), indicating the occurrence of chemical adsorption. Therefore, according to the results obtained from the thermodynamic and activation energy analysis, the process is endothermic, spontaneous, and chemical in nature.

From the results obtained, it is possible to simplify the GPR adsorption process in Figure 7.

**Figure 7.** Diagram adsorption mechanism.

3.6. Desorption Studies

Considering that the BY5G dye has a cationic nature and the zero charge point of granitic rocks is close to pH 7 [45], values below pH_{pcz} facilitate the desorption process. The test using NaOH solutions with pH values relative to pH_{pcz} showed desorption rates of 1.56% at pH 6 and 1.54% at pH 7. The behavior of distilled water was similar. Furthermore, for eluents with acidic pH values (pH 1 and 2), the desorption rates were 1.59% and 1.54%, respectively. The desorption rate resulting from the use of 50% (*v/v*) ethyl alcohol was 2.51%, which was the highest in relation to the other eluents and can be attributed to the ability of organic solvents to enter the active sites of the adsorbent owing to its low molecular weight, which consequently causes desorption [54].

The low desorption rates, even at favorable pH values for desorption, corroborate the E_a results, which indicate the occurrence of chemical adsorption, that is, the formation of chemical bonds between the adsorbate and adsorbent. Because of the low release of adsorbate in the liquid medium, the GRP after adsorption can be reused as a raw material in another production process without causing damage to the environment due to the release of dye. Given the crystallinity of the material indicated in the XDR test and the stability of the GRP with the BY5G dye, the material can be used as a filler in mortars and concrete to reduce the use of cement. Thus, the possibility of using GRP after adsorption in civil construction helps to minimize the waste generated by adsorption and enables

an adequate destination for the material, in addition to reducing the need for new raw materials, such as cement, as provided for in the circular economy.

3.7. Pozzolanic Activity Index (IAP) and Cement Performance Index

Regarding the analysis of the pozzolanicity of the material, the results of the IAP test indicated that the specification resistance was 0.30 MPa. NBR 12653 [55] establishes a minimum limit of 6.0 MPa to be considered a pozzolanic material. Therefore, this test demonstrated that the GRP after adsorption was inert. NBR 12653 [55] determines that for a material to be considered a pozzolan, a mortar with a 25% mineral addition must have a minimum resistance of 90% in relation to the reference mortar. Since the mortar with the addition of GRPA presented a compressive strength of 15.04 MPa (5.56% lower than the reference), it cannot be considered as pozzolanic and confirms the results found in the XDR and IAP. The classification of the GRP after adsorption as non-pozzolanic indicates the possibility of using it as a filler, as a nucleation point for cement hydration, and improving the compaction of the mixture, which can be evaluated by using tests with cement paste.

3.8. Physical Mechanical Characterization of Cement Pastes

Considering that the GRP after adsorption had filler characteristics, compressive and tensile strength tests by diametral compression with cement paste were used to measure the capacity of substituting the cement for the adsorbent material.

Regarding the compression test, the reference showed an average resistance of 24.88 MPa. The 5% and 10% substitutions resulted in strength increases of approximately 11.1% and 11.7%, respectively. The 15% replacement did not cause significant changes in the strength, whereas the 20% replacement caused a 17.76% drop in the compressive strength. In the tensile strength test, a 5%, 15%, and 20% substitution negatively affected this parameter, with a reduction of 20.5%, 13.4%, and 16.5%, respectively. However, the 10% replacement did not change the tensile strength compared to the reference. The results are shown in Figure 8.

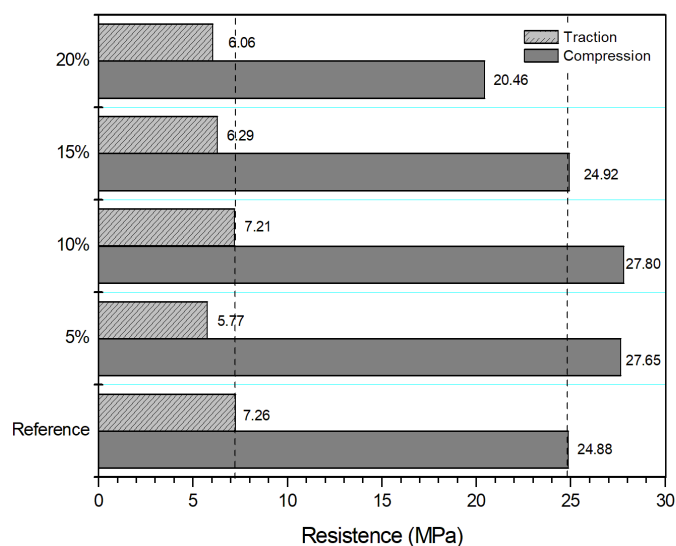


Figure 8. Compressive strength and tensile strength test with partial replacement of GRP after adsorption.

CP II–F cement tolerates a 25% mineral addition provided by NBR 16697 [56]. Considering that commercial cement has an average replacement of 10%, the addition of another 10% would result in a total addition of 20%, which is within the norm, and justifies the obtained results. Therefore, the 10% replacement was the one that presented the best results, proving to be the most adequate percentage for the incorporation of GRP after adsorption in mortars and with a potential application of the adsorbent material in civil

construction. This incorporation is beneficial because it reduces the need to use clinker in cement production and consequently reduces CO₂ emissions and production costs.

The voids and immersion absorption index in relation to the replacements carried out can be seen in Figures 9 and 10, respectively.

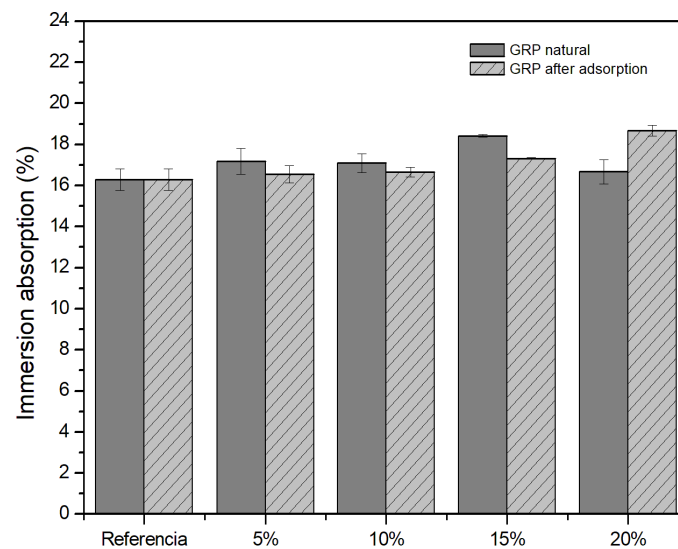


Figure 9. Immersion absorption for cement paste specimens.

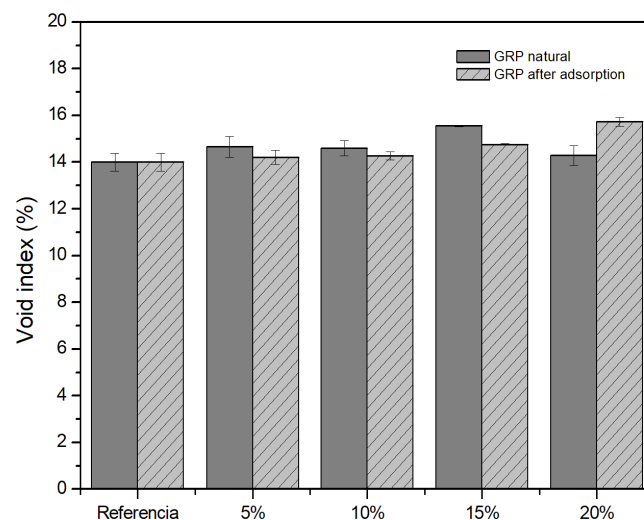


Figure 10. Void index for cement paste specimens.

The immersion absorption and void index values were higher than the reference values, with a gradually increasing trend for PRGA with increasing percentages. This behavior implies an increase in the porosity of the specimens, which is justified by the immersion absorption values and may be associated with a lower amount of clinker in the cement paste and the amount of water used to maintain the w/c ratio. The values found for replacing 15% of PRG and 20% of PRGA stand out, which demonstrate the highest values for the two parameters under analysis and resulted in lower values of compressive strength, demonstrating coherence between the results, since the increase in the number of voids generates a lower material resistance.

Considering the results of characterizing the reactivity of granite rock powder before and after adsorption, as well as studies on cement paste, it can be concluded that the material does not have pozzolanic activity and acts as a filler in mineral additions without significant effects on the loss of performance. The use of granite rock powder has

sustainable applications in different sectors. The use of powdery material as an adsorbent in the treatment of effluents, and the use of this residual adsorption material in the partial replacement of cement in mortars implies an alternative destination of the GRP and minimization of waste generated in the processes involved. Furthermore, its use as a filler in cement matrices reduces the demand for clinker, reducing the generation of polluting gases during cement production.

4. Conclusions

- Granitic rock powder proved efficient in removing BY5G dye from synthetic and industrial effluents.
- The adsorption mechanism was likely attributed to the Si-O group.
- The equilibrium time of the system decreases with the increasing temperature.
- The highest adsorption capacity was achieved at 323 K (18.52 mg g⁻¹).
- The adsorption process followed the pseudo-second-order kinetic model and the Langmuir isotherm.
- Negative ΔG° values indicate the spontaneity of the process, and positive ΔH° values suggest the endothermic nature of adsorption.
- The activation energy ($E_a = 71.35$ kJ mol⁻¹) and the low desorption rates imply chemical adsorption.
- GRP, both before and after adsorption, did not exhibit pozzolanic characteristics.
- There is a potential for using GRP as a partial replacement for cement in mortars.

Thus, the treatment of effluent containing the Basazol Yellow 5G dye using granitic rock powder can be considered a low-cost alternative because the material does not require pretreatment and is considered a waste due to the large amount produced. In addition, the process proved efficient, even at 298 K, showing great potential for industrial treatment in regions with similar temperatures. The possibility of using adsorption residual GRP as a filler is interesting for minimizing process residues, benefiting the environment and lowering production costs. The use of mining waste in alternative destinations increases the circularity of the material and consequently increases its useful life, making the process more sustainable and economical.

Author Contributions: Conceptualization, M.H.; methodology, M.H., E.P., L.N.B.d.A., R.J.E.M. and J.M.T.d.A.P.; validation, M.H., E.P. and J.M.T.d.A.P.; formal analysis, M.H., E.P., L.N.B.d.A., R.J.E.M. and J.M.T.d.A.P.; investigation, M.H.; data curation, M.H.; writing—original draft preparation, M.H. and J.M.T.d.A.P.; writing—review and editing, M.H., E.P., L.N.B.d.A., R.J.E.M. and J.M.T.d.A.P.; visualization, M.H., E.P., J.M.T.d.A.P. and L.N.B.d.A.; supervision, J.M.T.d.A.P. and E.P. All authors have read and agreed to the published version of the manuscript.

Funding: Coordenação de Aperfeiçoamento de Pessoal de Nível Superior—CAPES: 001.

Data Availability Statement: Data are contained within the article.

Acknowledgments: The authors thank CAPES for financial support, UTFPR—Ponta Grossa, IPB and UEPG for the structure and support provided for the development of the research.

Conflicts of Interest: The authors declare no conflict of interest.

References

1. FIEP. *Elementos de Economia Circular*; FIEP/PR: Curitiba, Brazil, 2019; p. 100. ISBN 978-85-61268-19-0.
2. Jorgensen, S.; Pedersen, L.J.T. The Circular Rather than the Linear Economy. *Restart Sustain. Bus. Model Innov.* **2018**, *1*, 103–120. [[CrossRef](#)]
3. Bellver-Domingo, Á.; Hernández-Sancho, F. Circular economy and payment for ecosystem services: A framework proposal based on water reuse. *J. Environ. Manag.* **2022**, *305*, 114416. [[CrossRef](#)] [[PubMed](#)]
4. Sarici, D.E.; Ozdemir, E. Utilization of granite waste as alternative abrasive material in marble grinding processes. *J. Clean. Prod.* **2018**, *201*, 516–525. [[CrossRef](#)]
5. Haldar, S.K. *Introduction to Mineralogy and Petrology*; Elsevier: Amsterdam, The Netherlands, 2020; Volume 2, ISBN 9780323851367.
6. Menossi, R.T.; Melges, J.L.P.; Akasaki, J.L.; Camacho, J.S.; Fazzan, J.V.; Tashima, M.M.; Salles, F.M. Pó de Pedra: Uma alternativa ou um complemento ao uso da areia na elaboração de misturas de concreto? *Holos Environ.* **2010**, *10*, 209–222. [[CrossRef](#)]

7. Dettmer, C.A.; Abreu, U.G.P.; Guilherme, D.O.; Neto, J.F.; Dettmer, T.L. *Uso de “Pó de Rocha” em Sistemas de Produção Agrícola: Breve Análise Sobre Viabilidade Técnica*; IV Encontro Internacional de Gestão, Desenvolvimento e Inovação: Navirai, Brazil, 2020; pp. 1–6.
8. Ramos, C.G.; Hower, J.C.; Blanco, E.; Oliveira, M.L.S.; Theodoro, S.H. Possibilities of using silicate rock powder: An overview. *Geosci. Front.* **2021**, *13*, 101185. [[CrossRef](#)]
9. Akar, N.A.S.; Abdel-Latif, M.L.; Sanad, S.A.; Mohammed, A.A.R. Utilization of industrial granitic waste as adsorbent for phosphate ions from wastewater. *Int. J. Sci. Eng. Res.* **2020**, *11*, 184–194.
10. Park, J.H.; Lee, J.K. Weathered Sand of Basalt as a Potential Nickel Adsorbent. *Processes* **2020**, *8*, 1238. [[CrossRef](#)]
11. Martínez, K.Y.; Toso, E.A.; Morabito, R. Production planning in the molded pulp packaging industry. *Comput. Ind. Eng.* **2016**, *98*, 554–566. [[CrossRef](#)]
12. Maeda, C.H.; Moretti, A.L.; Diório, A.; Braga, M.U.C.; Scheufele, F.B.; Barros, M.A.S.D.; Arroyo, P.A. The influence of electrolytes in the adsorption kinetics of reactive BF-5G blue dye on bone char: A mass transfer model. *Environ. Technol.* **2022**, 1–17. [[CrossRef](#)]
13. Knuston, K.P. *Enzymes Biobleaching Recalcitrant Paper Dye*; Institute of Paper Science and Technology at Georgia Institute of Technology: Atlanta, GA, USA, 2004; p. 345.
14. de Souza, R.M.; Quesada, H.B.; Cusioli, L.F.; Fagundes-Klen, M.R.; Bergamasco, R. Adsorption of non-steroidal anti-inflammatory drug (NSAID) by agro-industrial by-product with chemical and thermal modification: Adsorption studies and mechanism. *Ind. Crop. Prod.* **2021**, *161*, 113200. [[CrossRef](#)]
15. Borba, C.E.; Guirardello, R.; Silva, E.A.; Veit, M.T.; Tavares, C.R.G. Removal of nickel(II) ions from aqueous solution by biosorption in a fixed bed column: Experimental and theoretical breakthrough curves. *Biochem. Eng. J.* **2006**, *30*, 184–191. [[CrossRef](#)]
16. da Silva, B.C.; Zanutto, A.; Pietrobelli, J.M. Biosorption of reactive yellow dye by malt bagasse. *Adsorpt. Sci. Technol.* **2019**, *37*, 236–259. [[CrossRef](#)]
17. da Silva, D.C.C.; Pietrobelli, J.M.T.d.A. Residual biomass of chia seeds (*Salvia hispanica*) oil extraction as low cost and eco-friendly biosorbent for effective reactive yellow B2R textile dye removal: Characterization, kinetic, thermodynamic and isotherm studies. *J. Environ. Chem. Eng.* **2019**, *7*, 103008. [[CrossRef](#)]
18. Fairbairn, E.M.R.; De Paula, T.P.; Cordeiro, G.C.; Americano, B.B.; Filho, R.D.T. Evaluation of partial clinker replacement by sugar cane bagasse ash: CO₂ emission reductions and potential for carbon credits. *Rev. IBRACON Estrut. Mater.* **2012**, *5*, 229–251. [[CrossRef](#)]
19. Nakanishi, E.Y.; Frías, M.; Martínez-Ramírez, S.; Santos, S.F.; Rodrigues, M.S.; Rodríguez, O.; Savastano, H. Characterization and properties of elephant grass ashes as supplementary cementing material in pozzolan/Ca(OH)₂ pastes. *Constr. Build. Mater.* **2014**, *73*, 391–398. [[CrossRef](#)]
20. Assaad, J.J.; Vachon, M. Valorizing the use of recycled fine aggregates in masonry cement production. *Constr. Build. Mater.* **2021**, *310*, 125263. [[CrossRef](#)]
21. AlArab, A.; Hamad, B.; Chehab, G.; Assaad, J.J. Use of Ceramic-Waste Powder as Value-Added Pozzolanic Material with Improved Photocatalytic Performance. *J. Mater. Civ. Eng.* **2020**, *32*, 04020243. [[CrossRef](#)]
22. Isaia, G.C. *Concreto: Ciência e Tecnologia*; Instituto Brasileiro do Concreto (IBRACON): São Paulo, Brazil, 2011; Volume 1, pp. 261–309.
23. Fonseca, G.C. *Adições Mineraias e as Disposições Normativas Relativas à Produção de Concreto no Brasil: Uma Abordagem Epistêmica*; Programa de Pós-Graduação em Construção Civil, Universidade Federal de Minas Gerais: Belo Horizonte, Brazil, 2010.
24. Campos, H.F.; Rocha, T.M.S.; Reus, G.C.; Klein, N.S.; Filho, J.M. Determinação do teor ótimo de substituição do cimento Portland por pó de pedra usando métodos de empacotamento de partículas e análise do excesso de água na consistência de pastas. *Rev. IBRACON Estrut. Mater.* **2019**, *12*, 210–232. [[CrossRef](#)]
25. Ho, Y.S. Review of second-order models for adsorption systems. *J. Hazard. Mater.* **2006**, *136*, 681–689. [[CrossRef](#)]
26. Ho, Y.S.; McKay, G. Pseudo-second order model for sorption processes. *Process Biochem.* **1999**, *34*, 451–465. [[CrossRef](#)]
27. Tang, Y.; Chen, L.; Wei, X.; Yao, Q.; Li, T. Removal of lead ions from aqueous solution by the dried aquatic plant, *Lemna perpusilla* Torr. *J. Hazard. Mater.* **2013**, *244–245*, 603–612. [[CrossRef](#)] [[PubMed](#)]
28. Kumar, K.V.; Sivanesan, S. Prediction of optimum sorption isotherm: Comparison of linear and non-linear method. *J. Hazard. Mater.* **2005**, *126*, 198–201. [[CrossRef](#)] [[PubMed](#)]
29. AlArab, S.T.; Özcan, A.S.; Akar, T.; Kaynak, Z. Biosorption of a reactive textile dye from aqueous solutions utilizing an agro-waste. *Desalination* **2009**, *249*, 757–761. [[CrossRef](#)]
30. Akar, S.T.; Gorgulu, A.; Anilan, B.; Kaynak, Z.; Akar, T. Investigation of the biosorption characteristics of lead(II) ions onto *Symphoricarpus albus*: Batch and dynamic flow studies. *J. Hazard. Mater.* **2009**, *165*, 126–133. [[CrossRef](#)]
31. *ABNT NBR 5751*; Materiais Pozolânicos—Determinação da Atividade Pozolânica Com cal Aos Sete Dias. Associação Brasileira de Normas Técnicas (ABNT): Rio de Janeiro, Brazil, 2015.
32. *ABNT NBR 5752*; Materiais Pozolânicos—Determinação do Índice de Desempenho com Cimento Portland aos 28 dias. Associação Brasileira de Normas Técnicas (ABNT): Rio de Janeiro, Brazil, 2014.
33. *ABNT NBR 7215*; Cimento Portland—Determinação da Resistência à Compressão de Corpos de Prova Cilíndricos. Associação Brasileira de Normas Técnicas (ABNT): Rio de Janeiro, Brazil, 2019.
34. *ABNT NBR 7222*; Concreto e Argamassa—Determinação da Resistência à Tração por Compressão Diametral de Corpos de Prova Cilíndricos. Associação Brasileira de Normas Técnicas (ABNT): Rio de Janeiro, Brazil, 2011.

35. ABNT NBR 9778; Argamassa e Concreto endurecido—Determinação da Absorção de água, Índice de Vazios e Massa Específica. Associação Brasileira de Normas Técnicas (ABNT): Rio de Janeiro, Brazil, 2005.
36. Oliveira, E.; Bonk, B.; Felix, E.P.; Domingues, R.C.P.R. Adsorção de monóxido de carbono em carvão ativado convencional e impregnado com 5% de nióbio. *Matéria* **2021**, *26*, e13091. [[CrossRef](#)]
37. Mokrzycki, J.; Fedyna, M.; Marzec, M.; Szerement, J.; Panek, R.; Klimek, A.; Bajda, T.; Mierzwa-Hersztek, M. Copper ion-exchanged zeolite X from fly ash as an efficient adsorbent of phosphate ions from aqueous solutions. *J. Environ. Chem. Eng.* **2022**, *10*, 108567. [[CrossRef](#)]
38. Sing, K.S.W. Reporting physisorption data for gas/solid systems with special reference to the determination of surface area and porosity (Provisional). *Pure Appl. Chem.* **1982**, *54*, 2201–2218. [[CrossRef](#)]
39. Lopes, W.A.; Fascio, M. Esquema para interpretação de espectros de substâncias orgânicas na região do infravermelho. *Quim. Nova* **2004**, *27*, 670–673. [[CrossRef](#)]
40. da Silva, B.C.; Delgobo, E.S.; Corrêa, J.; Zanutto, A.; Medeiros, D.C.C.d.S.; Lenzi, G.G.; Matos, E.M.; Pietrobelli, J.M.T.d.A. Recovery of a synthetic dye through adsorption using malt bagasse, a by-product of brewing industry: Study in batch and continuous systems. *J. Water Process Eng.* **2023**, *56*, 104366. [[CrossRef](#)]
41. Mohamed, M.A.; Jaafar, J.; Ismail, A.F.; Othman, M.H.D.; Rahman, M.A. *Fourier Transform Infrared (FTIR) Spectroscopy, Membrane Characterization*; Elsevier: Amsterdam, The Netherlands, 2017. [[CrossRef](#)]
42. Wagh, P.B.; Kumar, R.; Patel, R.P.; Singh, I.K.; Ingale, S.V.; Gupta, S.C.; Mahadik, D.B.; Rao, A.V. Hydrophobicity Measurement Studies of Silica Aerogels using FTIR Spectroscopy, Weight Difference Method, Contact Angle Method and KF Titration Method. *J. Chem. Biol. Phys. Sci.* **2015**, *5*, 2350–2359.
43. Ramirez-Hernandez, C.; Aguilar-Flores, A. Aparicio-Saguilan, Fingerprint analysis of FTIR spectra of polymers containing vinyl análisis en la huella dactilar de espectros FTIR de polímeros que contienen etileno. *Rev. DYNA* **2019**, *86*, 198–205. [[CrossRef](#)]
44. Passaretti, M.G.; Ninago, M.D.; Paulo, C.I.; Petit, H.A.; Irassar, E.F.; Vega, D.A.; Villar, M.A.; Lopez, O.V. Biocomposites based on thermoplastic starch and granite sand quarry waste. *J. Renew. Mater.* **2019**, *7*, 393–402. [[CrossRef](#)]
45. Almeida, L.N.B.; Josue, T.G.; Nogueira, O.H.L.; Ribas, L.S.; Fuziki, M.E.K.; Tusset, A.M.; Santos, O.A.A.; Lenzi, G.G. The Adsorptive and Photocatalytic Performance of Granite and Basalt Waste in the Discoloration of Basic Dye. *Catalysts* **2022**, *12*, 1076. [[CrossRef](#)]
46. Luz, A.B.; Coelho, J.M. *Capítulo 19. Feldspato*; Rochas e Minerais Industriais—CETEM: Curitiba, Brazil, 2005; pp. 413–429.
47. Crini, G.; Peindy, H.N.; Gimbert, F.; Robert, C. Removal of C.I. Basic Green 4 (Malachite Green) from aqueous solutions by adsorption using cyclodextrin-based adsorbent: Kinetic and equilibrium studies. *Sep. Purif. Technol.* **2007**, *53*, 97–110. [[CrossRef](#)]
48. Benkhaya, B.; Harfi, S.E.; Harfi, A.E. Classifications, Properties and Applications of Textile Dyes: A Review. *Appl. J. Environ. Eng. Sci.* **2017**, *3*, 311–320. [[CrossRef](#)]
49. Fugaro, D.A.; Bruno, M. Remoção do azul de metileno de solução aquosa usando zeólitas sintetizadas com amostras de cinzas de carvão diferentes. *Quím. Nova* **2009**, *32*, 955–959.
50. Ren, B.; Jin, Y.; Zhao, L.; Cui, C.; Song, X. Enhanced Cr(VI) adsorption using chemically modified dormant *Aspergillus niger* spores: Process and mechanisms. *J. Environ. Chem. Eng.* **2022**, *10*, 106955. [[CrossRef](#)]
51. Giles, C.H.; Smith, D.; Huitson, A.A. General Treatment and Classification of the Solute Adsorption Isotherm I. Theoretical. *J. Colloid Interface Sci.* **1974**, *47*, 766–778. [[CrossRef](#)]
52. Eren, E.; Cubuk, O.; Ciftci, H.; Eren, B.; Caglar, B. Adsorption of basic dye from aqueous solutions by modified sepiolite: Equilibrium, kinetics and thermodynamics study. *Desalination* **2010**, *252*, 88–96. [[CrossRef](#)]
53. Fontana, K.B.; Chaves, E.S.; Sanchez, J.D.; Watanabe, E.R.; Pietrobelli, J.M.; Lenzi, G.G. Textile dye removal from aqueous solutions by malt bagasse: Isotherm, kinetic and thermodynamic studies. *Ecotoxicol. Environ. Saf.* **2016**, *124*, 329–336. [[CrossRef](#)]
54. Lu, P.J.; Lin, H.; Yu, W.; Chern, J. Chemical regeneration of activated carbon used for dye adsorption. *J. Taiwan Inst. Chem. Eng.* **2011**, *42*, 305–311. [[CrossRef](#)]
55. ABNT NBR 12653; Materiais Pozolânicos—Requisitos. Associação Brasileira de Normas Técnicas (ABNT): Rio de Janeiro, Brazil, 2014.
56. ABNT NBR 16697; Cimento Portland—Requisitos. Associação Brasileira de Normas Técnicas (ABNT): Rio de Janeiro, Brazil, 2018.

Disclaimer/Publisher’s Note: The statements, opinions and data contained in all publications are solely those of the individual author(s) and contributor(s) and not of MDPI and/or the editor(s). MDPI and/or the editor(s) disclaim responsibility for any injury to people or property resulting from any ideas, methods, instructions or products referred to in the content.